

**An analytical approximation for the macroscopic fundamental
diagram of urban traffic**

Carlos F. Daganzo and Nikolas Geroliminis

WORKING PAPER
UCB-ITS-VWP-2008-3



April 2008

An analytical approximation for the macroscopic fundamental diagram of urban traffic

Carlos F. Daganzo^{1*} and Nikolas Geroliminis²

¹ *Department of Civil and Environmental Engineering, University of California, Berkeley, USA*

² *Department of Civil Engineering, University of Minnesota, USA*

Abstract

This paper shows that a macroscopic fundamental diagram (MFD) relating flow and average density must exist on any street with blocks of diverse widths and lengths, but no turns, even if all or some of the intersections are controlled by arbitrarily timed traffic signals. The timing patterns are assumed to be fixed in time. Exact expressions in terms of a shortest path recipe are given, both, for the street's capacity and its MFD. Approximate formulas that require little data are also given.

Conditions under which the results can be approximately extended to networks encompassing large city neighborhoods are discussed. The MFD's produced with this method for the central business districts of San Francisco (California) and Yokohama (Japan) are compared with those obtained experimentally in earlier publications.

Keywords:

1. Introduction

It has been recently proposed (Daganzo, 2005, 2007) that traffic can be modeled dynamically in large urban regions (neighborhoods) at an aggregate level if the neighborhoods are uniformly congested and flows on their individual links exhibit fundamental diagrams (FD). The theory has already been tested with simulations and field experiments (Geroliminis and Daganzo, 2007, 2008). These tests unveiled that uniformly congested urban neighborhoods approximately exhibit a "Macroscopic Fundamental Diagram" (MFD) relating the number of vehicles (accumulation) in the neighborhood to the neighborhood's average speed (or flow), as required by the dynamic model. This happens even though the flow versus density plots for individual links exhibit considerable scatter.

**Corresponding Author: Phone: (510) 642-3853, Fax: (510) 642-1246
E-mails: daganzo@ce.berkeley.edu, nikolas@umn.edu*

According to this theory, the MFD is an approximate property of a network's structure that does not depend on demand. Thus, when estimated empirically, it gives decision-makers valuable information to evaluate demand-side policies for improving a neighborhood's mobility. However, to evaluate changes to the network (e.g., re-timing the traffic signals or changing the percentage of streets devoted to public service vehicles) one needs to know how the MFD is affected by the changes. To begin filling this gap, this paper explores the connection between network structure and the network's MFD for urban neighborhoods controlled at least in part by traffic signals. Traffic signals deserve special attention because on a signal-controlled link traffic delay for a given flow (and therefore the number of cars on the link) depends not just on the signal settings but also on the percentage of turns. Thus, an FD can at best only be defined approximately for a link controlled by a traffic signal: the scaling-up task may be challenging.

The challenge is compounded because we seek a universal recipe that can be used for all signal-controlled networks. However, recognizing that networks are complex structures described by many variables, we shall be satisfied with an approximation that uses as few of these variables as possible. The most similar work to what we propose is a simulation study (Gartner and Wagner, 2004) which, in the spirit of earlier works that examined the relationship between flow and density on rings (e.g. Wardrop, 1963; Franklin, 1967), explores how this relationship is affected by placing traffic signals on the ring. Gartner and Wagner (2004) simulated the ring for a limited range of signal timings and unveiled several regularities. These regularities, however, cannot be extrapolated to form a general theory because simulation only speaks to the range of simulated parameters. (An example of an unveiled regularity that cannot be extrapolated is the independence found between system capacity and signal offsets, which are known to be related when intersections are closely spaced.) In view of this, and given the many parameters required to describe a neighborhood, we shall take an analysis approach.

The paper is organized as follows: Section 2 first proves the existence and uniqueness of an exact, concave MFD for any multi-block, signal-controlled street without turning movements, using the tenets of variational theory (VT) (Daganzo, 2005a, b). This section also gives exact and approximate recipes for both, the street's capacity and its MFD. Section 3 then explains how, and under what conditions, the results can be scaled up approximately to complex networks. Finally, Section 4 compares the MFDs estimated for the networks of San Francisco (California, USA) and Yokohama (Japan) with those observed in Geroliminis and Daganzo (2007, 2008).

2. A single street with no turns

Considered here is a street of length L with a fixed number of lanes but any number of intersections. The intersections can be controlled by stop lines, roundabouts, traffic signals or any type of control that is time-independent on a coarse scale of observation; i.e. large compared with the signal cycles. We are interested in solutions where the flow at the downstream end of the street matches the flow at the upstream end; e.g. as if the street formed a ring, because then the average density does not change. To this end we will consider an initial value problem (IVP) on an extended version of our street, obtained as in Fig. 1 by placing end-to-end an infinite

number of copies of the original street. The problem will be treated with VT. We first show how to evaluate the capacity of this system; then turn our attention to the MFD.

2.1 Street capacity

The centerpiece of variational theory is a relative capacity (“cost”) function (CF) that describes each homogeneous portion of the street. This function gives the maximum rate at which vehicles can pass an observer moving with any given speed u ; its output has units of “flow”. We assume in this paper that the CF is linear, as shown in Fig. 2, and characterized by the following parameters: k_0 (optimal density), u_f (free flow speed), κ (jam density), w (backward wave speed), q_m (capacity), and r (maximum passing rate).

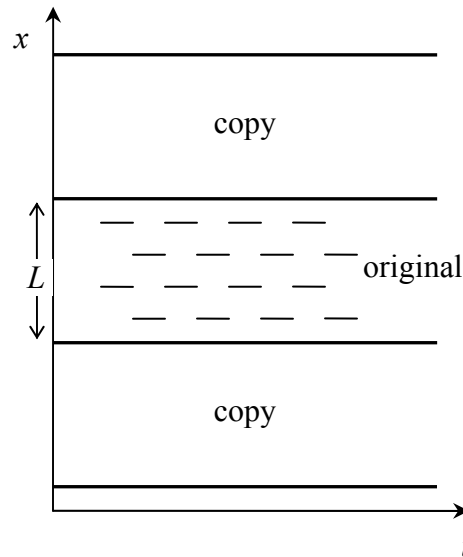


Figure 1: The periodic IVP for a single street of length L : short segments are red phases at intersections.

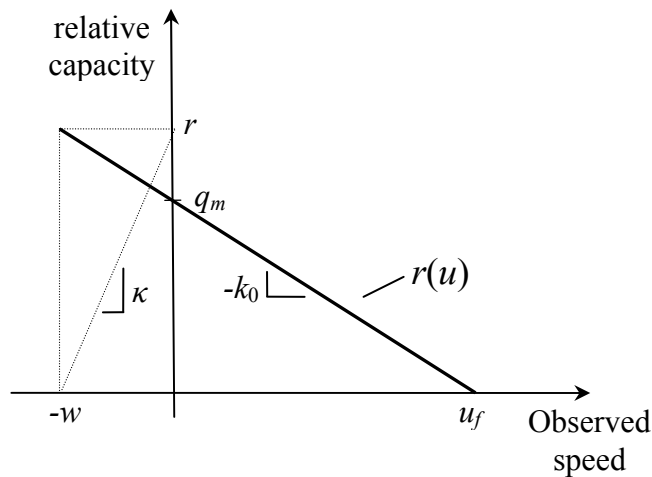


Figure 2: The linear cost function

In VT, the street can also have any number of time-invariant and/or time-dependent point bottlenecks with known capacities; e.g., at intersections controlled by traffic signals. The bottlenecks are modeled as lines in the t, x plane on which the “cost” per unit time equals the bottleneck capacity, $q_B(t)$. As an illustration, hypothetical red periods of signal-controlled intersections are indicated by short lines in the “original” swath of Fig. 1. These lines, replicated in all the copies, would have zero cost. During the green periods (G) the bottleneck capacity is the saturation flow of the intersection s , i.e., $q_B = s$, which could be equal or less than q_m .

A second element of VT is the set of “valid” observer paths on the (t, x) plane starting from arbitrary points on the boundary at $t = 0$ and ending at a later time, $t_0 > 0$. A path is “valid” if the observer’s average speed in any time interval is in the range $[-w, u_f]$. Let \mathcal{P} be one such path, $u_{\mathcal{P}}$ be the average speed for the complete path, and $\Delta(\mathcal{P})$ the path’s cost. This cost is evaluated with $r(u)$, treating any overlapping portions of the path with the intersection lines as shortcuts with cost $q_B(t)$. (Of course, $q_B = 0$ during the red periods.) By definition, $\Delta(\mathcal{P})$ bounds from above the change in vehicle number that could possibly be seen by observer \mathcal{P} . Thus, the quantity:

$$R(u) = \lim_{t_0 \rightarrow \infty} \inf_{\mathcal{P}} \{ \Delta(\mathcal{P}) : u_{\mathcal{P}} = u \} / t_0 \quad (1)$$

is an upper bound to the average rate at which traffic can overtake any observer that travels with average speed u for a long time. Note that (1) is a shortest path problem, and that $R(0)$ is the system capacity. Thus, the problem of evaluating the capacity of long heterogeneous streets with short blocks and arbitrary signal timings turns out to be conceptually quite simple.

It is also practically simple. It has been shown (Daganzo, 2005b) that for linear CF’s an optimal path always exists that is piece-wise linear: either following an intersection line or else slanting up or down with slope u_f or $-w$. This is illustrated by Fig. 3a, which depicts block i of our street (with length, l_i). In this figure arrows denote the possible directions of an optimal path, with associated costs shown in parentheses. Consideration shows that if all the blocks of our street are sufficiently long (such as the one in Fig. 3c) then the shortest path (SP) is a horizontal line along the trajectory of one of the intersections; and the capacity is simply: $R(0) = \min_i \{ s_i G_i / C_i \}$, where G_i is the effective green time and C_i the cycle time. However, if some of the blocks are short then there could be shortcuts that use red periods at more than one intersection, as shown in Fig. 3b. In this case the capacity is smaller.

Example: As an illustration, we evaluate the capacity, c , of a homogeneous ring road with two diametrically opposed and identically timed signals. Let $2l$ be the length of the road, and assume $s = q_m$. We only consider the two symmetric cases where the offsets are the same for both signals: $\delta = 0$ and $\delta = C/2$. In order to obtain a complete solution with as few degrees of freedom as possible, we choose the units of time, distance and vehicular quantity so that $C = 1$, $u_f = 1$ and $s = 1$, and evaluate the capacity for all possible combinations of the remaining parameters: G, l, δ .

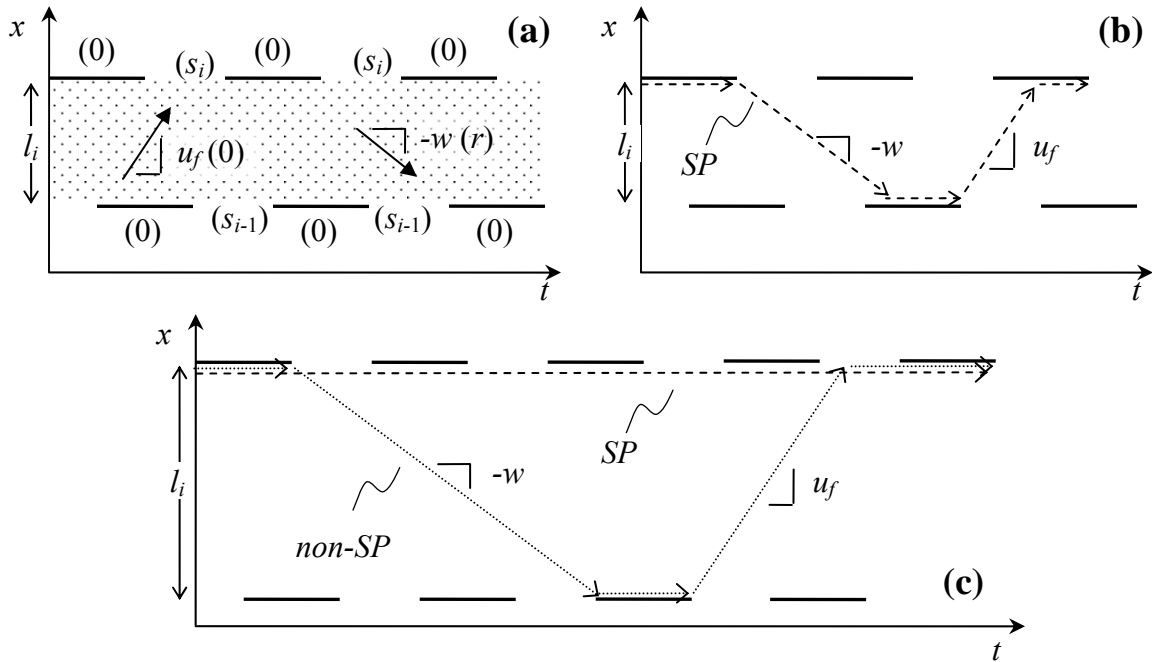


Figure 3: Estimation of capacity according to VT: (a) costs; (b) short block; (c) long block

The reader can verify using the shortest path method described above that the complete solution to this problem is as displayed in Fig. 4. This solution matches the known capacity formulae for pairs of intersections. Note that offsets affect capacity considerably when blocks are short: $l < G$. Appendix A gives capacity formulae for a few additional cases.

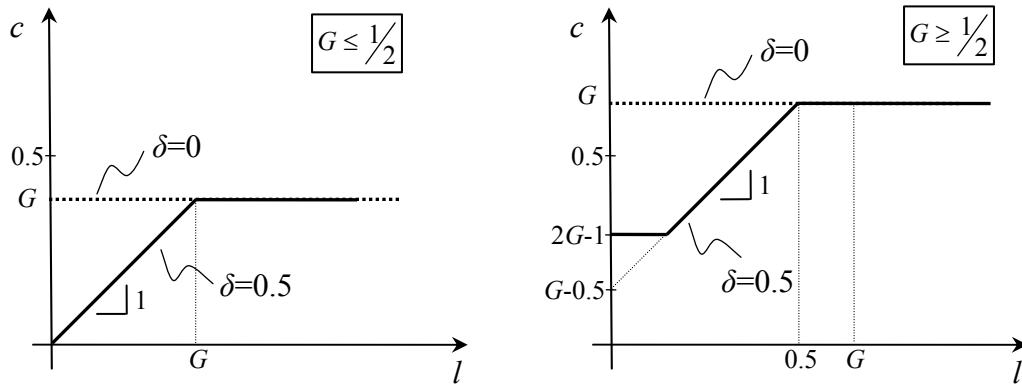


Figure 4: Capacity of a symmetric ring with two signals

2.2 The street's MFD

Consider now an IVP with a periodic initial density, with average k . This problem is known to have a unique solution with meaningful densities everywhere (Daganzo, 2006) and, since all its input data are periodic in space, this solution must be periodic -- with period L . Thus, our original street has the same inflows and outflows: it behaves as a ring, as desired.

Consider next the average flow from $t = 0$ to $t = t_0$ at some location (say $x = 0$), and denote it by $q(t_0)$. Because our IVP is periodic so that vehicles are conserved, $q(t_0)$ approaches a location-independent limit, q , as $t_0 \rightarrow \infty$. This limit will, of course, depend on the initial density distribution. We now show that q is connected with the initial density distribution only through its average; i.e., that an MFD function Q , $q = Q(k)$, exists. We also show that Q is concave.

PROPOSITION: *A ring's MFD, $q = Q(k)$, is concave and given by:*

$$q = \inf_u \{ku + R(u)\}. \quad (2)$$

Proof: Recall from VT that the vehicle number at a point is the greatest lower bound of the numbers that could have been computed by all valid observers, \mathcal{P} , by adding each observer's $\Delta(\mathcal{P})$ to its given initial number (at the boundary). We now evaluate with this recipe the vehicle number, n_0 , observed when $t = t_0 \rightarrow \infty$ at the location where the initial vehicle number is 0. We do this by considering observers ending their trips at the location in question but traveling with different long term average speeds u (and of course emanating from different points on the boundary). By using (1) and noting that the initial vehicle number for an observer with average speed u is in the range $ku t_0 \pm \kappa L$ we find that $n_0 \pm \kappa L = \inf_u \{ku t_0 + R(u)t_0\}$, where $t_0 \rightarrow \infty$. Thus, on dividing both sides by $t_0 \rightarrow \infty$ we obtain (2). To conclude the proof we need to show that (2) is concave. But this is clear because (2) is the lower envelope of a set of straight lines, which is always a concave curve. \square

The term $R(u)$ can be obtained with the SP recipe of Sec. 2.1. Figure 5 illustrates that (2) is the lower envelope of the 1-parameter family of lines on the (k, q) plane defined by $q = ku + R(u)$ with u as the parameter. We call these lines “cuts” because they individually impose constraints of the form: $q \leq ku + R(u)$ on the macroscopic flow-density pairs that are feasible on our street. This inequality should be intuitive, since it is well known that an observer traveling at speed u in a traffic stream (k, q) is passed at a rate q_r such that $q = ku + q_r$, and we showed in Sec 2.1 that $q_r \leq R(u)$. Less obvious is that according to our proposition there always is a “tight” cut that yields the average flow for any given density, such as those shown for k_1 , k_2 and k_3 in the figure.

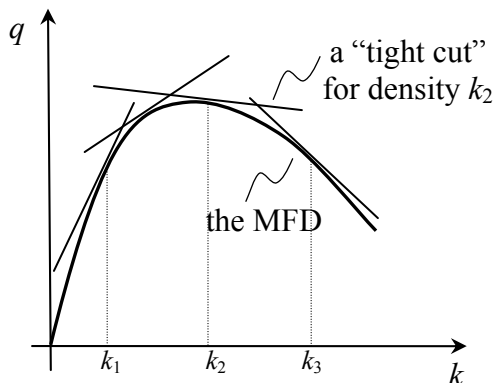


Figure 5: The MFD defined by a 1-parameter family of “cuts”

2.3 Practical approximations

Because evaluating $R(u)$ in (2) for all u can be tedious, we propose instead using three families of “practical cuts” that jointly bound the MFD from above, albeit not tightly. The approximate MFD is denoted by T instead of Q . Note T is concave, and $T \geq Q$. Our practical cuts are based on observers that can move with only 3 speeds: $u = u_f$, 0, or $-w$. Recall that an observer’s cost rate is $q_B(t)$ if the observer is standing at intersection with capacity $q_B(t) \leq q_m$ and otherwise it is as given by Fig. 2; i.e., it is either 0, s or r .

Family 1: The first family uses stationary observers at different locations, and out of these, we choose the one standing at the most constraining intersection. This leads to the first cut:

$$q \leq q_B = \min_i \{s_i G_i / C_i\}, \quad (3)$$

where q_B is the average capacity of the most constraining intersection.

Family 2: Now consider observers that move forward at speed u_f , except where delayed by a red phase at an intersection. Assume that all the red phases R_i have been extended at the front end by an amount εG_i , where $\varepsilon \in [0,1]$ is a parameter. (The delayed observer always departs the intersection at the end of the red, even when $\varepsilon = 1$.) Let $u(\varepsilon)$ be the average speed of this observer and $f_i(\varepsilon)$ the fraction of time that it spends stopped in green phases of intersection i (and its copies) because of extended reds. This observer can be passed at most at rate s_i during $f_i(\varepsilon)$, and not at all other times. Thus, traffic can pass it on average at a rate $q_r \leq \sum_i s_i f_i(\varepsilon)$ on average, and the moving observer formula yields our second family of cuts:

$$q \leq ku(\varepsilon) + \sum_i s_i f_i(\varepsilon), \quad \text{for } 0 \leq \varepsilon \leq 1. \quad (4a)$$

If the street is homogeneous, with the same q_m on all its blocks ($q_m \geq s_i$), one may use the rougher cut:

$$q \leq ku(\varepsilon) + q_m f(\varepsilon), \quad \text{for } 0 \leq \varepsilon \leq 1, \quad (4b)$$

where $f(\varepsilon) = \sum_i f_i(\varepsilon)$ is the fraction of time that the vehicle is stopped on extended red phases.

Family 3: The third and last family is the mirror image of the second, with the observer traveling in the opposite direction, at speed w instead of u_f , and also stopping for the red phases. Now we use $w(\varepsilon) > 0$ for the average speed of the observer, $b_i(\varepsilon)$ for the fraction of time it spends in extended red phases of intersection i and $h_i(\varepsilon)$ for the fraction of time it spends moving toward i . This observer can be passed at most at rate r_i when moving. Therefore, it can be passed in total at most at an average rate $\sum_i [s_i b_i(\varepsilon) + r_i h_i(\varepsilon)]$, so that the resulting set of cuts arising from the moving observer formula is:

$$q \leq -kw(\varepsilon) + \sum_i [s_i b_i(\varepsilon) + r_i h_i(\varepsilon)], \quad \text{for } 0 \leq \varepsilon \leq 1. \quad (5a)$$

Again, if the street is homogeneous, with the same q_m and r on all its blocks, one may prefer to use the rougher cut:

$$q \leq -kw(\varepsilon) + q_m b(\varepsilon) + r \frac{w(\varepsilon)}{w}, \quad \text{for } 0 \leq \varepsilon \leq 1, \quad (5b)$$

where $b(\varepsilon) = \sum_i b_i(\varepsilon)$ is the fraction of time that the observer is stopped on extended red phases, and $w(\varepsilon)/w = \sum_i h_i(\varepsilon)$ is the fraction of time that the observer is moving.

Equations (4) and (5) can be further simplified for any homogeneous street (i.e., with uniform block lengths and signal settings), because in this case the observers follow simple periodic paths with one stop per period. These paths only differ in the number of blocks, $\gamma = 1, 2 \dots \gamma_{max}$, traversed per stop, where γ_{max} may be infinite. Therefore, γ can be used as a (discrete) parameter instead of ε . Using this approach, Appendix B expresses all the cuts (4-5) of a homogeneous street in terms of l , G , C , and the offset δ .

How good are these simplifications? The reader can verify without too much effort that for the symmetric ring of Sec. 2.1 the five simple cuts given by (3) and the two extreme cases of (4b) and (5b) (with $\gamma = 1$ and $\gamma = \gamma_{max}$) define an approximate MFD, T , with a capacity that matches exactly the one predicted in Sec. 2.1. Furthermore, it is possible to show that these five simple cuts always predict exactly the capacity of a homogeneous street with two signals.¹ Therefore, we conjecture that (3-5) should be good approximations in general. They will be the basis for our numerical tests.

3. Application to urban areas

Three complexities now arise. First, unlike our ring, real urban streets never contain a perfectly invariant number of vehicles – even in a steady state – because these vehicles can both, randomly turn at intersections and either begin or finish their trips along the street itself. Second, these turns and trip ends violate the tenets of VT. And third, route choice should be considered. We address the last two issues first because taken together they simplify matters.

3.1 Turns, trip ends and route choice

We conjecture that on highly redundant networks (e.g., grids) on which people make trips that are long compared with a city block, the average speeds “ v ” on street portions that are geographically close should themselves be close. This conjecture is plausible on the basis of driver navigation habits (e.g., Wardrop, 1952). We also assume that the network can be roughly partitioned into streets, j , that over a relevant period of observation (say 30 min) roughly satisfy the properties of Sec. 2 – i.e., have small *net* average (in)outflows along their lengths due to turns and trip ends. Under these conditions, each of these streets should exhibit (approximately) a well defined MFD, Q_j . Then, it turns out that the results of Sec. 2 can be preserved.

¹ The reason is geometric. Consideration shows that for $t_0 \rightarrow \infty$ a least cost path with zero average speed (which defines the capacity of our system) can always be constructed by splicing together a subset of our five elementary paths.

To see this, let $q_j = F_j(v_j)$ be a street's speed-based MFD, which we define as usual by means of the transformations: $v_j = q_j/k_j$ and $F_j(q_j/k_j) = Q_j(k_j)$. We also define an approximate speed-based MFD, $q_j = V_j(v_j)$, by means of the same transformation of $T_j(k_j)$. Note that $F_j(v) \leq V_j(v)$ for all v , since $Q_j(k_j) \leq T_j(k_j)$. Speed-based MFDs are advantageous because if speeds are similar in all used parts of the network we can use the inequality $F_j(v) \leq V_j(v)$, with the prevailing speed as an input, to bound the flow on each street individually: $q_j = F_j(v) \leq V_j(v)$.

Furthermore, we can also bound the average neighborhood flow which we define as in Daganzo (2005) by: $q = \sum_j q_j L_j / D$, where L_j is the length of street j and D the total length of the network. Clearly now, since $q_j = F_j(v) \leq V_j(v)$, we have:

$$q = \sum_j q_j L_j / D \leq \sum_j V_j(v) L_j / D \equiv V(v) \quad (6)$$

This shows that for a given average neighborhood speed, the average neighborhood flow should be bounded from above by a function, $V(v)$, which is the weighted average of the speed-based MFD's of all the neighborhood streets. This approximation should be good if the network speeds are uniform and our MFD bound is tight. Furthermore, if the streets are similar, then any of the V_j 's (or Q_j 's) can be used to approximate the whole neighborhood.

3.2 Statistical fluctuations

Here we propose a second order approximation to capture the statistical effects induced by both, turns and trip ends. Experience with simulations and real-life shows that random variations in trip-making can create spatial pockets where the average speed and accumulation are temporarily different from the prevailing average. These localized differences should be temporary in neighborhoods with constant demand due to the effects of route choice. But, despite the stabilizing effect of route choice, both speed and density must be distributed over space at any given time with some dispersion -- even if their long term averages are the same everywhere. We now examine how the dispersion in density affects the long term average flow.

Since traffic is granular and random (even in the steady state) the vehicular input and output to any given street or link behaves as a superposition of binomial processes, so that the number of vehicles in it fluctuates from the average as a random walk. We are interested in the distribution of these fluctuations over space, conditional on the total number of vehicles in the network, n . If the stabilization effects of route choice are so strong that they prevent large pockets of congestion from developing, but yet are weak enough to allow for significant excursions from the average on individual links (which seems reasonable) we would expect the n vehicles to be randomly distributed among links i in proportion to the number of available positions, $N_i \equiv \kappa_i l_i$. Thus, we propose modeling the number of vehicles on a link with the hypergeometric distribution, as if available positions were chosen without replacement by the circulating vehicles. And, since our networks have many links we use the binomial approximation instead (as if sampling with replacement). Then, if we express the number of vehicles on link i as a

dimensionless “concentration”, $\rho_i = k_i/\kappa_i \in [0, 1]$, and use ρ for the (given) concentration of the network, we should have:

$$E(\rho_i) = \rho \quad \text{and} \quad \text{var}(\rho_i) \approx \rho(1-\rho)/N_i, \quad (7)$$

Since $N_i \sim 10^1$ to 10^2 for typical links, we see that the coefficient of variation of ρ_i can range from 15% to 45% when $\rho \sim 0.3$ (a value close to capacity). For this range of variation, the normal approximation is appropriate.

If the local fluctuations in density persist for times substantially longer than a signal cycle, they should affect the average network flow as per:

$$q \cong E[Q(\rho_i\kappa)] \leq E[T(\rho_i\kappa)]. \quad (8)$$

Note that $E[Q(\rho_i\kappa)] \leq Q(k)$ and $E[T(\rho_i\kappa)] \leq T(k)$ because Q and T are concave. Thus, the effect of granularity slightly reduces network flows.

4. Applications

4.1 The study sites

We apply the described methodology to estimate an MFD of two study sites. The first site is simulated and the second real. The first site provides a controlled test that isolates the errors of the proposed approximation. The second site merely illustrates how the method may work in a real-world application where the assumptions of the model are slightly violated and the input data includes some error. For more information about the study sites and the experiments see Geroliminis and Daganzo (2007, 2008).

The first test site is a 5 km² area of Downtown San Francisco (Financial District and South of Market Area), including about 100 intersections with link lengths varying from 100 to 400m. Traffic signals are pre-timed with a common cycle. Network geometry and traffic flow data were available from previous studies.

The second site is a 10 km² part of downtown Yokohama. It includes streets with various numbers of lanes and closely spaced signalized intersections (100-300m). Major intersections are centrally controlled by actuated traffic signals that effectively become pre-timed (with a common cycle) during the rush.

4.2 Results

Although both sites are somewhat heterogeneous we treat them as if they could be decomposed into sets of homogeneous 1-lane streets, similar within each city; e.g., by visualizing multi-lane streets as side-by-side juxtapositions of 1-lane streets. Therefore we use the simplified version of (6) in which the MFD of a single typical street is used (a 1-lane street in our case). This is a very rough approximation, but it simplifies the task at hand since it allows us to use the formulae of

Appendix B. Only the following information is needed: (i) network variables, D (network length in lane-km) and l (average link length); (ii) link variables (for 1-lane), $s = q_m$, κ , w and u_f ; and (iii) intersection variables, δ , C and G . Table I summarizes the values of all input parameters for the two study sites. Recall that the San Francisco (SF) site is a simulated network with pre-timed control and we have exact information for signal settings, offsets and geometries. These were not available for the Yokohama (Y) site.

All the SF parameters, except $u_{\gamma_{max}}$, γ_{max} , q_B , G and w , were inputs to the micro-simulations in Geroliminis and Daganzo (2007, 2008). Therefore, they were chosen here to match. The exceptions were resolved as follows: $u_{\gamma_{max}}$ was estimated by simulating the network with very light traffic ($\sim 10^1$ vehicles circulating); γ_{max} by solving (B2) and (B3) with the estimated $u_{\gamma_{max}}$; q_B as the simulated average queue discharge rate per lane from all the signals; G with $G = q_B C / G$; and w as per Fig. 2 with $w = u_f / (\kappa u_f / q_m - 1)$.

For Yokohama, real-world data were used. Parameters D and l were estimated from road maps; C , κ and q_m were reported by local experts (Kuwahara, 2007); speeds u_f and $u_{\gamma_{max}}$ from vehicle GPS data; q_B from detector data; and γ_{max} , G and w as in SF. Note that the Yokohama site includes traffic responsive signal control; thus, the offsets calculated for light conditions are not representative of the whole. Since no additional information given, we assumed that signals operate synchronously when traffic is moderate, e.g., near the peaks. This corresponds to an offset of 0 sec.

	Site 1 (SF)	Site 2 (Y)
u_f (m/sec)	13.4	13.9
$u_{\gamma_{max}}$ (m/sec)	7.0	8.4
γ_{max}	4	5(peak)
D (km)	76.2	157.0
l (m)	122.9	154.0
κ (vh/m)	0.13	0.14
q_m (vh/sec)	0.5	0.5
q_B (vh/sec)	0.175	0.190
w (m/sec)	5.4	5.0
δ (sec)	2.6	0 (peak)
G (sec)	21	49
C (sec)	60	130

Table 1: Parameters of the model

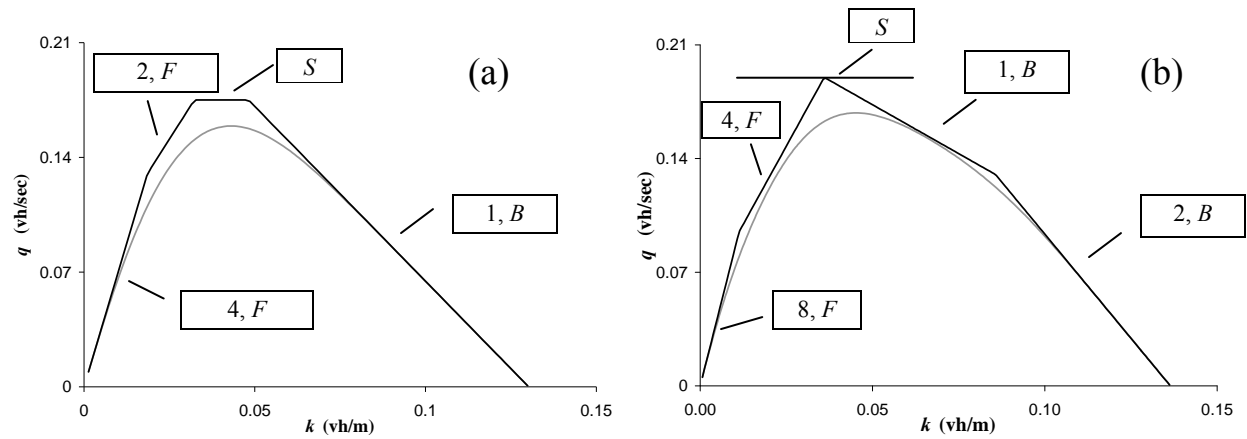


Figure 6: Theoretical MFD with and without stochastic variations: (a) San Francisco, (b) Yokohama

With these data, MFDs were constructed for both cities using the three types of cuts for all $\gamma = 1, 2 \dots \gamma_{max}$. The piecewise linear curves of Figure 6 show the result: only tight cuts are shown. The two entries in each box are the value of γ and the observer type (F for forward, B for backward, S for stationary). The smooth grey curve is the granular approximation (8).

Figures 7a and 7b compare the speed-based MFDs obtained from the granular approximations in Figs. 6a and 6b with those reported in Geroliminis and Daganzo (2007). For the SF site of Fig. 7a, each point represents the city's average speed and accumulation every 5 min. Even though very different spatial and temporal demand patterns were simulated, the city-wide average speeds are consistent and closely predicted.

Fig. 7b includes more error but this was not surprising because: (i) Yokohama used actuated signals with settings that varied with time; (ii) its network is less homogeneous; and (iii) our input data comes from field observation and expert opinion (not simulation) which may include significant error. The errors induced by (i) could have been alleviated by estimating different MFD's for different times of the day; the errors induced by (ii) by using more than one street type in (6); and the errors due to (iii) by a comprehensive field study. Unfortunately, the data required for these refinements were not available.

In summary, it appears that a neighborhood's MFD can be approximately predicted from data that encapsulate key network characteristics. Although improvements and extensions of the proposed approximation should be sought, it can already be used to explore roughly but systematically the connection between a city's mobility and the structure of its streets and control system.

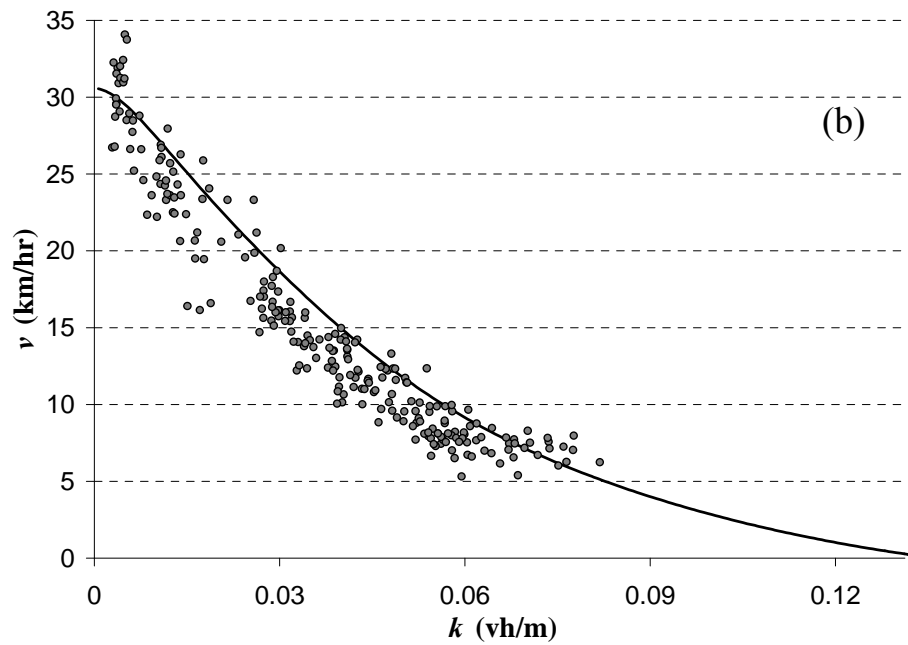
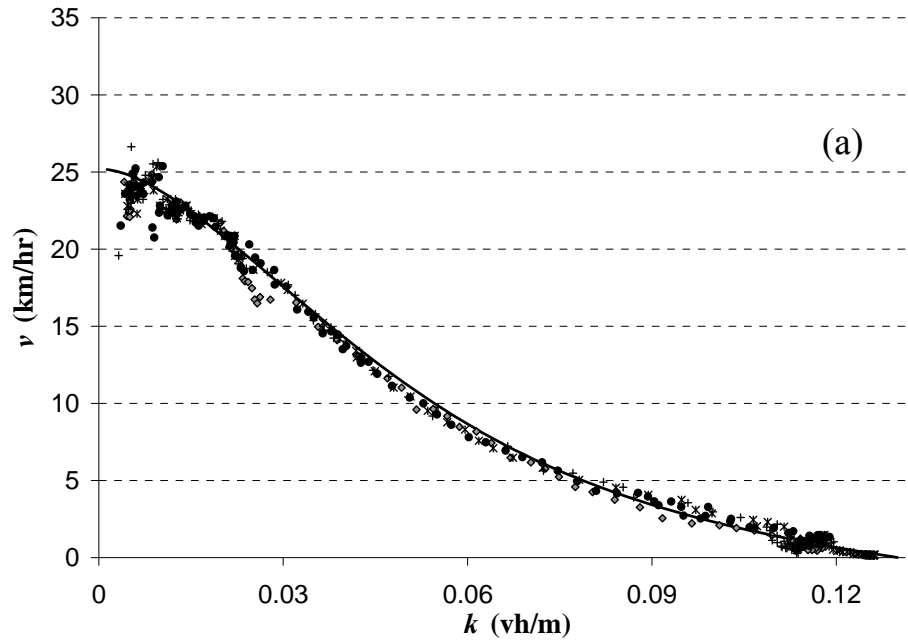


Figure 7: Estimated MFD: (a) San Francisco, (b) Yokohama

Appendix A: Capacity formulae for some special cases

Here we give capacity formulas for some special cases where the calculations are simple.

Unsignalized intersections with 4-way stops: They can be modeled as signals with very short cycles: letting $G_j, C_j \rightarrow 0$ while holding G_j/C_j constant and using a proper value for s_j . Then, $q_{B_j} = s_j \cdot G_j / C_j$.

Pairs of intersections: There are several cases with simple results.

Case 1: Neighboring unsignalized intersections ($C_j = C_{j-1} \rightarrow 0$). In this case shortcuts do not exist and $q_B = \min\{q_{B_j}, q_{B_{j-1}}\}$.

Case 2: Neighboring signalized and unsignalized intersections ($C_j = 0$ and $C_{j-1} > 0$ or vice versa). Assume that $s = q_m$ (zero turns). Let (C, G) be the timing parameters of the signalized intersection and $g = q_{B_j}/q_m$ the equivalent fraction of green for the unsignalized intersection. Then, if $g \geq G/C$ (the signal is more restrictive) we have:

$$\text{(Short block) } \kappa l < q_m G : q_B = (l\kappa + g(Gq_m - l\kappa))/C \quad (\text{A1})$$

$$\text{(Long block) } \kappa l \geq q_m G : q_B = q_m G/C \quad (\text{A2})$$

Case 3: Properly timed signals with a common cycle: If there is a common cycle an offset always exist that guarantees the same system capacity as if $l_j = \infty$, e.g., the offset $\delta = 0$ (This is a well known result and can be verified with VT). Thus, for properly timed signals: $q_B = \min\{q_{B_j}, q_{B_{j-1}}\}$.

Case 4: Improperly timed signals (different cycles): Also of interest is the case where $C_j \approx C_{j-1} \approx C$ but $C_j \neq C_{j-1}$. In this case, the offsets vary approximately uniformly between 0 and C and we find:

$$q_B \approx \frac{l\kappa}{C} + \frac{1}{2} \left(\frac{Gq_m}{C} - \frac{l\kappa}{C} \right). \quad (\text{A3})$$

In summary, for cases 2, 3 and 4 above, we have:

$$q_B = \frac{l\kappa}{C} + \alpha \left(\frac{Gq_m}{C} - \frac{l\kappa}{C} \right) \quad \text{if } \kappa l \geq Gq_m \text{ (short block)} \quad (\text{A3})$$

$$= Gq_m / C \quad \text{o.w.} \quad (\text{A4})$$

where $\alpha = 1/2$ for improperly timed signals, $\alpha = g \geq G/C$ when one of the intersections is unsignalized (but not restrictive) and $\alpha = 1$ if signals have favorable offsets or the block is long. Cases not covered by equations A3 and A4 can be evaluated with the VT recipe.

Appendix B: A cut for deterministic offsets

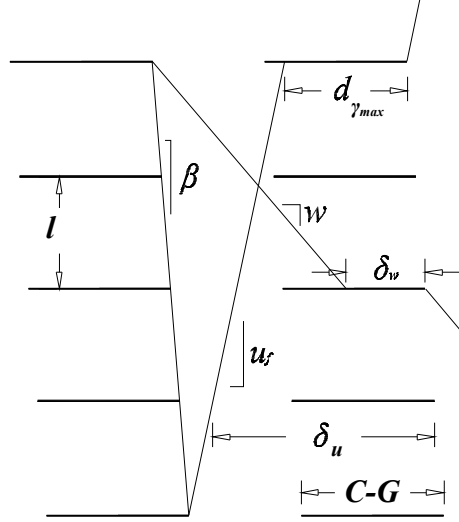


Figure B1: Time-space diagram for $\delta > C - G$ and $\delta_w < C - G$

The object of study is a street with uniform block length, l , and signal settings (offset δ , C and G). Consider first an observer that travels at free flow speed, u_f , and stops only when the signal turns red. Note that no car can overtake this observer. To express our formulae, it will be convenient to work with the “relative offset” δ_u instead of δ . The relative offset (see figure) is the absolute offset one would have had if the timing pattern of the upstream signal had been shifted forward in time by l/u_f time units. If this observer stops because of a traffic signal every γ_{max} links, it will experience the following delay:

$$d_{\gamma_{max}} = C - \gamma_{max} l / \beta - \gamma_{max} l / u_f \quad (\text{B1})$$

where β is ($\beta > 0$ in case of figure B1):

$$\beta = \frac{l}{C - \delta_u - l / u_f} \quad (\text{B2})$$

The average speed of this observer is:

$$u_{\gamma_{max}} = \frac{\gamma_{max} l}{d_{\gamma_{max}} + \gamma_{max} l / u_f} = \frac{\gamma_{max} l}{C - \gamma_{max} l / \beta} \quad (\text{B3})$$

Note that for perfectly timed signals ($\gamma_{max} \rightarrow \infty$), $u_{\gamma_{max}} = u_f$. Consideration of figure B1 shows that

$$\gamma_{max} = \max \left\{ \gamma : \gamma (L / u_f + L / \beta) / C - \lfloor \gamma (L / u_f + L / \beta) / C \rfloor \leq (C - G) / C \right\} \quad (\text{B4})$$

Consider now a slower observer who stops every γ signals ($\gamma=1, 2, \dots, \gamma_{max}-1$) because of extended red phases, as described in Sec 2.3. The speed and delay of this observer are given by (B1) and (B3) after replacing γ_{max} by γ for $\gamma = 1, 2, \dots, \gamma_{max} - 1$. The fraction of time that it spends in extended red phases f_γ is:

$$f_\gamma = \frac{d_\gamma - C + G}{C - \gamma l / \beta} \quad (B5)$$

Equations (B1)-(B4) also hold for backward moving observers (Family 3 in Sec 2.3). For this observer we define a relative offset, δ_w , as shown by the figure. We see by symmetry that the observer's speed $w(\varepsilon)$ and delay are still given by (B1), (B2), (B3) and (B4) after replacing u_f by w and δ_u by δ_w ; and that the fraction of time stopped in extended red phases, $b(\varepsilon)$, is still given by (B5). Thus, (5b) can now be applied.

References

- Daganzo, C.F., 2005a. Improving city mobility through gridlock control: an approach and some ideas, Working Paper UCB-ITS-VWP-2005-1, U.C. Berkeley Center of Excellence on Future Urban Transport, University of California, Berkeley, CA.
- Daganzo, C.F., 2005b. A variational formulation of kinematic waves: Basic theory and complex boundary conditions, *Transportation Research Part B* 39(2), 187-196.
- Daganzo, C.F., 2005c. A variational formulation of kinematic waves: Solution methods, *Transportation Research Part B* 39(10), 934-950.
- Daganzo, C.F., 2006. On the variational theory of traffic flow: well-posedness, duality and applications, *Networks and Heterogeneous Media* 1(4) 601-619 (2006).
- Daganzo, C.F., 2007. Urban gridlock: macroscopic modeling and mitigation approaches, *Transportation Research part B* 41, 49-62.
- Edie, L.C., 1963. Discussion of traffic stream measurements and definitions, Proc. 2nd Int. Symposium on the Theory of Traffic Flow, (J. Almond, editor), pp. 139-154, OECD, Paris, France.
- Franklin, R.E., 1967. Single-lane traffic flow on circular and straight tracks, in *Vehicular Traffic Science*, Proc. 3rd International Symposium on the Theory of Traffic Flow (L.C. Edie, R. Herman and R. Rothery, editors) pp.42-55.
- Gartner N. and Wagner P., 2004. Analysis of Traffic Flow Characteristics on Signalized Arterials, In *Transportation Research Record: Journal of the Transportation Research Board*, No. 1883, 94-100.

Geroliminis, N. and C.F. Daganzo, 2007. Macroscopic modeling of traffic in cities, *86th Annual Meeting of the Transportation Research Board*, paper # 07-0413, Washington DC.

Geroliminis, N. and C.F. Daganzo, 2008. Existence of urban-scale macroscopic fundamental diagrams: some experimental findings, *Transportation Research Part B* (in press); see also Working Paper UCB-ITS-VWP-2007-5, U.C. Berkeley Center of Excellence on Future Urban Transport, University of California, Berkeley, CA.

Lighthill, M.J. and J.B. Whitham, 1955. On kinematic waves. I. Flow movement in long rivers. II. A theory of traffic flow on long crowded road, *Proceedings of the Royal Society A* 229, 281-345.

Kuwahara M. , 2007. Private communication

Mahmassani, H., Williams, J., Herman, R., 1987. Performance of urban traffic networks, in Proc. 10th Int. Symposium on the Theory of Traffic Flow, (Gartner N. and Wilson N. editors), pp. 1-20, MIT, Cambridge, US.

Richards, P.I., 1956. Shockwaves on the highway, *Operations Research*, 22, 81-101.

Smeed, R. J., 1966. Road Capacity of City Centers, *Traffic Engineering and Control*, 8(7), 455-458.

Wardrop, J.G., 1952. Some theoretical aspects of road traffic research, *Proc. Inst. Civ. Eng., Part II*, 1(2), 325-362; Discussion, 362-378.

Wardrop, J.G., 1965. Experimental speed/flow relations in a single lane, in Proc. 2nd International Symposium on the Theory of Road traffic Flow, (J. Almond, editor), pp. 104-119, OECD, Paris, France.